# Multiple Magnon Modes and Consequences for the Bose–Einstein Condensed Phase in $BaCuSi_2O_6$

Ch. Rüegg,[1,*] D. F. McMorrow,[1,2] B. Normand,[3] H. M. Rønnow,[4] S. E. Sebastian,[5]
I. R. Fisher[5] C. D. Batista,[6] S. N. Gvasaliya,[4] Ch. Niedermayer,[4] and J. Stahn[4*]
[1] *London Centre for Nanotechnology; Department of Physics and Astronomy; University College London; London WC1E 6BT; UK*
[2] *ISIS Facility; Rutherford Appleton Laboratory; Chilton; Didcot OX11 0QX; UK*
[3] *Institute of Theoretical Physics; Ecole Polytechnique Fédérale de Lausanne; 1015 Lausanne; Switzerland*
[4] *Laboratory for Neutron Scattering; ETH Zurich and Paul Scherrer Institute; 5232 Villigen PSI; Switzerland*
[5] *Geballe Laboratory for Advanced Materials and Department of Applied Physics; Stanford University; Stanford CA 94305; USA*
[6] *Condensed Matter and Statistical Physics; Los Alamos National Laboratory; Los Alamos; USA*
(Dated: February 6, 2008)

The compound $BaCuSi_2O_6$ is a quantum magnet with antiferromagnetic dimers of $S = 1/2$ moments on a quasi–2D square lattice. We have investigated its spin dynamics by inelastic neutron scattering experiments on single crystals with an energy resolution considerably higher than in an earlier study. We observe multiple magnon modes, indicating clearly the presence of magnetically inequivalent dimer sites. This more complex spin Hamiltonian leads to a distinct form of magnon Bose–Einstein condensate (BEC) phase with a spatially modulated condensate amplitude.

PACS numbers: 75.10.Jm; 78.70.Nx; 05.30.Jp

The investigation of field–induced quantum phase transitions (QPTs) in magnetic insulators continues to enrich our understanding of the possible quantum ground states of matter [1, 2, 3, 4, 5]. Structurally dimerized quantum spin systems play a preeminent role in these studies. One recent example is the phase diagram of the compound $BaCuSi_2O_6$ [6, 7, 8, 9], in which antiferromagnetic dimers formed by the $S = 1/2$ magnetic moments from pairs of $Cu^{2+}$ ions are arranged on a quasi–two–dimensional (2D) square lattice. This material is one of the best candidates for the investigation of field–induced BEC of magnetic quasiparticles, and a 3D–2D dimensional crossover at the QPT has been reported [9].

The ground state of weakly interacting antiferromagnetic dimers is a spin singlet ($|S, S_z\rangle = |0, 0\rangle$) separated by an energy gap $\Delta$ from excited triplet states ($|1, 0\rangle$ and $|1, \pm 1\rangle$). A QPT occurs at the field $H_c = \Delta/g\mu_B$, where the $S_z = +1$ component condenses. At $H > H_c$ the average triplet density becomes finite (magnon BEC) and the ground state changes from a nonmagnetic singlet to an ordered magnetic phase. The triplet quasiparticles may also be considered as hard–core bosons with a kinetic energy and an effective repulsion. Depending on the balance between these terms, a characteristic spatial modulation of the triplet density may arise, whereas in a uniform BEC this is identical for all sites.

The classes of field–induced QPT known to date in dimer spin systems are summarized in Fig. 1. For magnetic interactions with weak or no frustration, the kinetic energy is dominant and the ordered, or BE–condensed, ground state is uniform at $H > H_c$, as in $TlCuCl_3$ [4, 5, 10, 11]. In $SrCu_2(BO_3)_2$ [5, 12, 13] triplet hopping is suppressed by geometrical frustration and the repulsion causes the condensed triplets to form a superlattice with spontaneous breaking of translational symmetry and the appearance of magnetization plateaus [14]. All dimer sites have finite, if weak, triplet density at $H > H_c$ [13]. Magnetization plateaus occur also for strong and explicit translational symmetry breaking, which leads to inequivalent dimer sites and multiple magnon modes, as in $NH_4CuCl_3$ [15, 16] where the separation of the singlet–triplet gaps exceeds the magnon band widths.

Prior to this study the magnetic Hamiltonian used to describe $BaCuSi_2O_6$ was based on an inelastic neutron scattering (INS) investigation with coarse energy resolution [6] and on fits to thermodynamic data [7, 8]. Motivated by the exotic low–temperature behavior [9], the lack of high–resolution data and reports of a structural phase transition around 100 K [17, 18], we have investigated the magnetic excitation spectrum by high–resolution INS. We find explicitly broken translational symmetry in the form of structurally inequivalent dimer sites, which produces a BEC with spatial modulation of the triplet density, but without magnetization plateaus. As a consequence our conclusions extend beyond the determination of the spin Hamiltonian to demonstrate that $BaCuSi_2O_6$ represents a fourth category [Fig. 1(IV)] of spatially modulated BEC system, and we propose a closer examination of the magnetic properties around the field–induced quantum critical point (QCP).

Five single crystals of $BaCuSi_2O_6$ were coaligned to provide a total mass of 1.25 g. The total mosaic spread of the assembly was excellent and matched the instrumental resolution [Fig. 2(a)]. A tetragonal–to–orthorhombic distortion occurring below $T \approx 100$ K was detected very recently by high–resolution x–ray diffraction [18]. The small difference between $a$– and $b$–axes is related to a structural modulation with wave vector (0 0.129 0); crys-

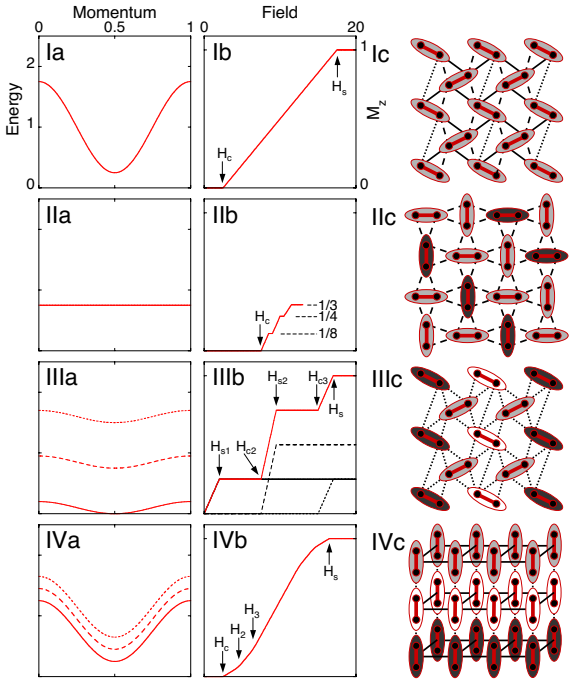


FIG. 1: Physical properties at a field–induced QPT in dimer–based $S = 1/2$ spin systems. (a) triplet dispersion at zero field, (b) uniform magnetization $M_z$, (c) dimer lattice with triplet condensate amplitude for $H > H_c$ represented by increasing grey scale. (I) 3D systems with uniform magnon BEC, e.g. $TlCuCl_3$. (II) Shastry–Sutherland geometry with magnetization plateaus and strong contrast in condensate amplitude, e.g. $SrCu_2(BO_3)_2$ (field in panel (c) yielding $M_z = 1/3$). (III) Same features for 3D system with strong translational symmetry–breaking and weak interdimer interactions, e.g. $NH_4CuCl_3$ at $H_{c2} < H < H_{s2}$. (IV) Quasi–2D system on square lattice with weakly broken translational symmetry showing no magnetization plateaus, e.g. schematic model for $BaCuSi_2O_6$ at $H_c < H < H_3$.

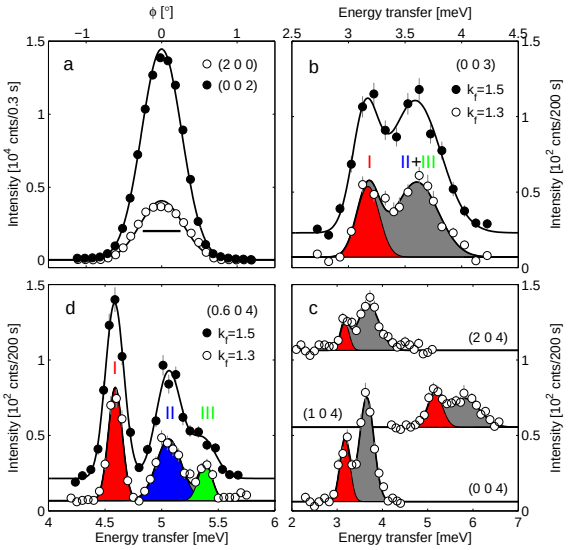


FIG. 2: (a) Rocking curves across two Bragg peaks of coaligned $BaCuSi_2O_6$ sample. Horizontal line indicates instrumental resolution (full width) of neutron diffractometer MORPHEUS. (b–d) INS spectra of $BaCuSi_2O_6$ at $T = 1.8$ K and $H = 0$ T, experimental conditions as indicated. Momentum vectors in reciprocal lattice units (r.l.u.) of tetragonal space group $I4_1/acd$ with $a = b = 10.01$ Å and $c = 22.47$ Å [17], i.e. $(q_h\ 0\ 4)$ is diagonal direction on square lattice.

tals are twinned below this transition [18], which should result in spatial averaging of in–plane properties.

INS spectra at $T = 1.8$ K and zero magnetic field were collected on the cold–neutron triple–axis spectrometer TASP [19], operated with fixed final momentum $k_f = 1.3$ Å$^{-1}$ (1.5 Å$^{-1}$), focusing Pyrolytic Graphite monochromator and analyzer, cold Be filter, and open horizontal collimation to gain intensity. The Gaussian energy resolution of 0.14(0.23) meV (FWHM) is considerably improved compared to that in Ref. [6]. Figure 2(b) shows the spectrum at the AF zone center $\boldsymbol{Q}$=$(q_h\ q_k\ q_l)$=(0 0 3) and can be compared directly to Fig. 2(b) of Ref. [6]. Surprisingly, the singlet–triplet gap has a clear multi–peak structure over an energy range of 1 meV. This splitting cannot be attributed to the multi–crystal sample [Fig. 2(a)], being observed consistently in different instrumental configurations including flat analyzer, and confirmed on different instruments (below). We conclude that the triplet excitation spectrum of $BaCuSi_2O_6$ shows intrinsically more features than originally reported.

The INS spectrum in Fig. 2(b) is described adequately by two Gaussian peaks. However, while the excitation at lower energy transfer, denoted henceforth as mode I, has an energy width compatible with the instrumental resolution, the peak at higher energies is considerably broader. The evolution of the inelastic signal in the square–lattice plane is presented in Fig. 2(c), and the multi–peak structure is observed at every point. At (0.6 0 4) the slope of the resolution ellipsoid matches that of the dispersion relation, giving optimal resolution conditions [Fig. 2(d)]: this spectrum reveals that the excitation at higher energy transfer consists of at least two transitions, which are denoted as modes II and III. However, peak II remains broader in energy than expected from the instrumental resolution (cf. mode I), and therefore may consist of more than one mode.

The energy dispersion of modes I–III is extracted from the data by least–squares fits of the resolved peaks, and is summarized in Figs. 3(a) and (b). A cosine dispersion is observed in the square–lattice plane: modes I–III disperse in parallel and are well described by the lowest–order perturbative expression

$$\begin{aligned} E_\alpha(\boldsymbol{Q}) = J_\alpha &- J'_\alpha(\cos(\pi q_h + \pi q_k) + \cos(\pi q_h - \pi q_k)) \\ &+ J''_\alpha(\cos(2\pi q_h) + \cos(2\pi q_k)) \\ &+ 2J^f_\alpha \cos(\tfrac{\pi}{2} q_l)|\cos(\pi q_h) - \cos(\pi q_k)|, \end{aligned} \quad (1)$$

where $\alpha = 1, 2, 3$ denotes modes I–III. Parameters $J_\alpha$

are intradimer interactions, with $J'_\alpha$ and $J''_\alpha$ respectively nearest– and next–nearest–neighbor in–plane interdimer interactions and $J^f_\alpha$ the effective interlayer interactions. The measured energies have no detectable $q_l$–dependence (bandwidth below 0.05 meV), confirming previous claims that $BaCuSi_2O_6$ is quasi–2D. This is a consequence of the frustrated geometry of the interlayer coupling [inset Fig. 3(b)], and the precise determination of $J^f_\alpha$ is deferred to a future experiment. Here we take $J^f_\alpha = 0$, consistent with the fact that the other parameters in Eq. (1) correspond to decoupled planes and no more general model is required. A fit to the complete data set gives dominant intradimer interactions $J_1 = 4.27(1)$, $J_2 = 4.72(1)$, and $J_3 = 5.04(4)$, with $J'_1 = 0.49(1)$, $J'_2 = 0.52(1)$, $J''_1 = -0.07(1)$, and $J''_2 = -0.03(1)$, all in meV; we take $J'_3 = \frac{1}{2}(J'_1 + J'_2)$ and $J''_3 = \frac{1}{2}(J''_1 + J''_2)$ to approximate the dispersion of mode III. Thus we find in contradiction to Ref. [6] that the only significant interdimer interactions are those forming the square lattice, $J'_\alpha \approx 0.1 J_\alpha$. The individual gaps at the AF zone center are $\Delta_1 = 3.15(5)$, $\Delta_2 = 3.62(5)$, and $\Delta_3 = 3.94(8)$ meV.

The total INS intensity of modes I–III is modulated along (0 0 $q_l$) by the dimer structure factor $|f(\boldsymbol{Q})|^2 \sin(dq_l)^2$ [6] [Fig. 3(d)], with $2d = 2.85(6)$ Å the average projected intradimer separation and $f(\boldsymbol{Q})$ the magnetic form factor of $Cu^{2+}$. However, fitting intensities I and II+III separately gives $2d_I = 2.52(18)$ Å and $2d_{II+III} = 2.99(10)$ Å [Fig. 3(d)], a difference indicative of inequivalent dimer layers, as already suggested by the multi–mode dispersion. However, a model with uniform layers of dimer oriented parallel to the $c$–axis and modulated only in this direction would predict a weakly decreasing INS intensity with increasing $|(q_h\ 0\ 4)|$. The $q_h$–dependence of the measured intensity [Fig. 3(c)] shows further structure which is clearly inconsistent with equivalent dimer sites in each plane [and thus also with the simple representations in Fig. 1(IVc) and Eq. (1)]. We are forced to conclude that the magnetic interactions are also modulated within the square planes, consistent with what is known of the low–temperature structure [18], as well as between adjacent planes.

The dependence of the excitation spectrum on magnetic fields up to $H = 4$ T is shown for the resolution–focusing point in Fig. 4. These data were collected on the spectrometer RITA–II [20] with experimental conditions similar to TASP. The $H = 0$ T data in Fig. 4(a) confirm our conclusions concerning the multi–peak excitation structure [cf. Fig. 2(d)]. At finite magnetic fields a redistribution of spectral weight is observed. While mode I is clearly split, the transitions at higher energies are barely resolved due to peak overlap [Figs. 4(b,c)]. One may proceed by fixing the peak widths at the zero–field values and redistributing the spectral weight according to the relative contributions expected for Zeeman–split triplet modes, namely 1/4, 1/2, and 1/4 respectively for $S_z = +1, 0$, and $-1$ components; the only fitting parameters are the centers of the Gaussian peaks. This approach describes the observed finite–field spectra quite satisfactorily, whereas a model with field–independent modes II and III cannot [dashed lines in Figs. 4(b,c)]. Fits of individual energies, $\tilde{E}_{\alpha,}$ and a common $g$–factor are summarized in Fig. 4(d): $\tilde{E}_1 = 4.58(1)$ meV, $\tilde{E}_2 = 5.06(1)$ meV, and $\tilde{E}_3 = 5.39(1)$ meV [cf. Fig. 2(d)], while $g = 2.01(4)$, in good agreement with the value reported in Ref. [8]. That each of the modes I–III displays individual Zeeman splitting into components $E^{\pm,0}_\alpha(H)$ demonstrates again the presence of inequivalent dimer sites. Different candidate mechanisms for a zero–field energy splitting, such as exchange anisotropy or Dzyaloshinskii–Moriya interactions [10, 21], are probably present in $BaCuSi_2O_6$ at some small energy scale [22]. However, these would produce only three modes at finite fields and are therefore excluded as the origin of our observations.

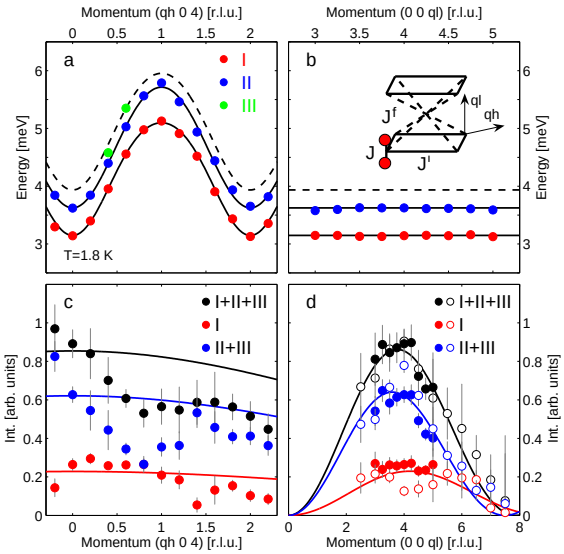


FIG. 3: (a–b) Triplet dispersion in $BaCuSi_2O_6$ at zero field and $T = 1.8$ K: (a) in–plane along $\boldsymbol{Q}$=($q_h$ 0 4), (b) perpendicular to plane with $\boldsymbol{Q}$=(0 0 $q_l$) (see inset). (c–d) Momentum–dependence of (scaled) INS intensity, with solid lines as described in text: total intensity modes I–III (black), mode I (red), and modes II+III (blue) measured with $k_f = 1.3$ Å$^{-1}$ (solid circles) and 1.5 Å$^{-1}$ (open circles).

The INS results presented here identify $BaCuSi_2O_6$ in a class of low–dimensional quantum magnets which has not yet been considered: despite explicitly broken translational symmetry of the spin Hamiltonian there are no plateaus in the uniform magnetization (Fig. 1) [7]. Both the presence of four dimer layers along the $c$–axis of the large unit cell and the structural distortion at $T \approx 100$ K introduce the potential for different intra– and interdimer interactions. Our results indicate that both interlayer and weak in–plane modulations are present, and that these are due most likely to differential dimer tilts away from the $c$–axis. A minimal magnetic model could

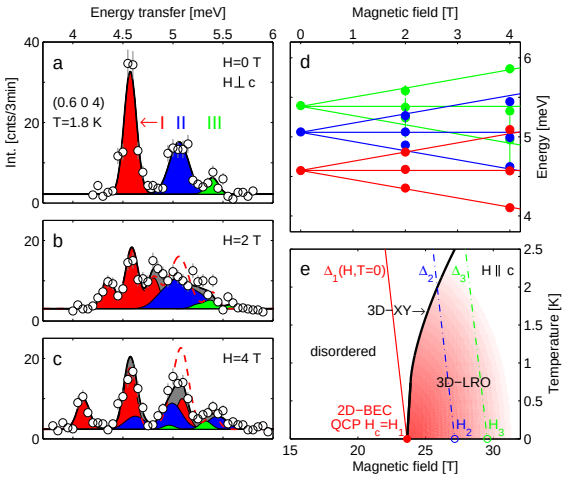


FIG. 4: (a–c) INS spectra at three magnetic–field values in $BaCuSi_2O_6$ for $\boldsymbol{Q}$=(0.6 0 4), $T$ = 1.8 K, and $k_f$ = 1.3 Å$^{-1}$. (d) Zeeman splitting of triplet modes following procedure described in text. (e) Schematic phase diagram around QPT; intensity of red shading indicates qualitative degree of $c$–axis modulation of BEC order parameter.

be expected to generate at least 4 excitations, consistent with the broad, unresolved appearance of mode II.

The inequivalent dimer sites reflected in the INS spectra result in gaps $\Delta_\alpha$ which differ by less than the band widths of the individual triplets, in contrast to $NH_4CuCl_3$ [16] [Figs. 1(IIIa,IVa)], removing the possibility of magnetization plateaus [Figs. 1(IIIb,IVb)]. Each of the measured modes shows Zeeman splitting in an applied field, which would drive the spin system towards a QCP occurring when the lowest gap $\Delta_1$ vanishes at $H_1 = H_c$. Above $H_c$, the density of triplet quasiparticles would be largest for sites of type $\alpha = 1$, but because of their direct real–space coupling, dimers of types $\alpha = 2$ and 3 would also acquire finite, if weak, triplet densities [13, 15]. The BEC state must therefore be characterized by a spatially modulated amplitude of the order parameter. As the field is increased through the values $H_\alpha$ corresponding to the gaps $\Delta_\alpha$ ($\alpha = 2$ and 3), raising the uniform magnetization and the BEC order parameter, the effect of interdimer interactions in a system such as $BaCuSi_2O_6$ is to cause a mixing of the low–lying triplet modes $E^+_\alpha(H)$ with the ground state. This mixing precludes further phase transitions and causes the magnetization to display a crossover rather than a kink at these fields [Fig. 1(IVb)], in accord with the measurement of Ref. [7]. The spatial modulation of the BEC order parameter may in principle be detected by nuclear magnetic resonance (NMR) studies of the many inequivalent Cu sites at $H > H_c$ [23].

In $BaCuSi_2O_6$ our results indicate that the dimer modulation occurs predominantly between planes [Figs. 3(c,d)], and thus that the indices $\alpha$ correspond to separate bilayers. In this case the triplet density at $H_c < H < H_2$ is higher on dimer layers $\alpha = 1$, and is lower on the intervening bilayers [cf. Fig. 1(IVc)]; indeed the structural modulation must lead in this way to an enhancement of the anisotropic nature of the BEC order parameter, as depicted in Fig. 4(e). The structural modulation also raises the distinct possibility that geometrical frustration of interlayer triplet hopping [Eq. (1)] is less than perfect at low temperatures. However, the thermodynamic measurements of a 2D QCP in $BaCuSi_2O_6$ as a consequence of this frustration [9] demonstrate that the energy scale of any unfrustrated hopping component is below 30 mK.

In summary, we have investigated the magnetic excitation spectrum of $BaCuSi_2O_6$ in zero field and at $H < H_c$ by inelastic neutron scattering on single crystals. The very much higher energy resolution than in earlier studies allows the determination of a spin Hamiltonian whose exchange interactions indicate a complex picture of the ground state and of the field–induced QPT observed in this material. Inequivalent dimer sites give a multi–mode excitation spectrum, and as a further consequence the BEC phase at $H > H_c$ is anticipated to be spatially modulated. Although INS studies are currently limited to 17 T $< H_c$, high–field magnetization and NMR experiments could explore in greater detail the modulated BEC phase whose characteristic features are predicted here.

We thank N. Harrison, M. Jaime and R. Stern for valuable discussions. This work is based on experiments performed at the Swiss spallation neutron source SINQ, Paul Scherrer Institute, Villigen, Switzerland. The project was supported by the Swiss National Science Foundation and by the US National Science Foundation, Division of Materials Research, under grant DMR-0134613.

* Electronic address: c.ruegg@ucl.ac.uk

[1] I. Affleck, Phys. Rev. B **43**, 3215 (1991).
[2] T. Giamarchi, and A.M Tsvelik, Phys. Rev. B **59**, 11398 (1999).
[3] S. Sachdev, *Quantum Phase Transitions* (Cambridge University Press, Cambridge, UK, 1999).
[4] T. Nikuni, M. Oshikawa, A. Oosawa, and H. Tanaka, Phys. Rev. Lett. **84**, 5868 (2000).
[5] T.M. Rice, Science **298**, 760 (2002).
[6] Y. Sasago, K. Uchinokura, A. Zheludev, and G. Shirane, Phys. Rev. B **55**, 8357 (1997).
[7] M. Jaime et al., Phys. Rev. Lett. **93**, 087203 (2004).
[8] S.E. Sebastian et al., Phys. Rev. B **72**, 100404(R) (2005).
[9] S.E. Sebastian et al., Nature **441**, 617 (2006).
[10] Ch. Rüegg et al., Nature **423**, 62 (2003).
[11] M. Matsumoto, B. Normand, T.M. Rice, and M. Sigrist, Phys. Rev. Lett. **89**, 077203 (2002); Phys. Rev. B **69**, 054423 (2004).
[12] H. Kageyama et al., Phys. Rev. Lett. **82**, 3168 (1999).
[13] K. Kodama et al., Science **298**, 395 (2002).
[14] M. Oshikawa, M. Yamanaka, and I. Affleck, Phys. Rev. Lett. **78**, 1984 (1997).

[15] M. Matsumoto, Phys. Rev. B **68**, 180403(R) (2003).
[16] Ch. Rüegg et al., Phys. Rev. Lett. **93**, 037207 (2004).
[17] K.M. Sparta, and G. Roth, Acta Cryst. B **60**, 491 (2004).
[18] E.C. Samulon et al., Phys. Rev. B **73**, 100407(R) (2006).
[19] F. Semadeni, B. Roessli, and P. Böni, Physica B **297**, 152 (2001).
[20] K. Lefmann et al., Physica B **283**, 343 (2000).
[21] V.N. Glazkov, A.I. Smirnov, H. Tanaka, and A. Oosawa, Phys. Rev. B **69**, 184410 (2004).
[22] S.E. Sebastian et al., Phys. Rev. B, in press.
[23] M. Horvatic et al., Prog. Theor. Phys. Suppl. **159**, 106 (2005).